AGU PUBLICATIONS

Geophysical Research Letters

RESEARCH LETTER
10.1002/2017GL073379

Spacecraft measurements constraining the spatial extent of a magnetopause reconnection X line

B. M. Walsh[1], **C. M. Komar**[2], **and Y. Pfau-Kempf**[3]

[1]Mechanical Engineering Department and Center for Space Physics, Boston University, Boston, Massachusetts, USA, [2]Geospace Physics Laboratory, NASA Goddard Space Flight Center, Greenbelt, Maryland, USA, [3]Department of Physics, University of Helsinki, Helsinki, Finland

Key Points:
- Magnetic reconnection is observed to be active at one point and inactive elsewhere along the dayside magnetopause
- Magnetopause reconnection can have a finite extent in local time

Correspondence to:
B. M. Walsh,
bwalsh@bu.edu

Citation:
Walsh, B. M., C. M. Komar, and Y. Pfau-Kempf (2017), Spacecraft measurements constraining the spatial extent of a magnetopause reconnection X line, *Geophys. Res. Lett.*, *44*, doi:10.1002/2017GL073379.

Received 7 MAR 2017
Accepted 25 MAR 2017
Accepted article online 29 MAR 2017

Abstract Multispacecraft measurements from the Time History of Events and Macroscale Interactions during Substorms (THEMIS) mission are used to probe the spatial extent of an X line at the dayside magnetopause. A case study from 21 April 2014 is presented where two THEMIS spacecraft have a near-simultaneous encounter with the equatorial dayside magnetopause separated by 3.9 Earth radii. Both spacecraft observe similar steady inflow conditions with southward interplanetary magnetic field and a high magnetic shear angle at the magnetopause (133°) boundary. One spacecraft observes clear fluid and kinetic signatures of active magnetic reconnection, while the other spacecraft does not observe reconnection. The predicted location of reconnection across the magnetopause is found using several theoretical models and a Block Adaptive Tree Solarwind Roe-type Upwind Scheme (BATS-R-US) MHD simulation. Each model predicts a continuous X line passing close to the two spacecraft, suggesting both would observe reconnection, if active. Using the constraints of the multipoint measurements, the extent or length L of the reconnection is estimated to be $2.4 \leq L < 5.2$ h in local time or $6 \leq L < 14\ R_E$.

1. Introduction

The behavior and structure of magnetic reconnection has been often studied in the plane of reconnection; however, the structure of the process in the direction normal to the reconnection plane has received less attention. For southward interplanetary magnetic field (IMF), and applications at the Earth's magnetopause, the extent in the direction normal to the reconnection plane corresponds to the extent of reconnection in local time. Whether the X line is continuous or patchy and what controls the extent of an X line at the dayside magnetopause remain open questions that are of importance both for solar wind-magnetospheric coupling and for our fundamental understanding of the reconnection process.

One possibility is that reconnection could be a spatially continuous and extended process. Multipoint measurements in the solar wind have shown evidence for spatially continuous reconnection [*Phan et al.*, 2006a; *Gosling et al.*, 2007a] extending as much as 4×10^6 km [*Gosling et al.*, 2007b]. Consistent with measurements in the solar wind, extended X lines have also been inferred from spacecraft at the Earth's magnetopause. Simultaneous detection by spacecraft with separation of multiple hours in local time provides evidence for an extended and potentially continuous X line across the dayside magnetopause [*Phan et al.*, 2000, 2006b; *Dunlop et al.*, 2011; *Walsh et al.*, 2014; *Hasegawa et al.*, 2016]. Similar conclusions of a long extended X line across the magnetopause have also been made based auroral observations [*Fuselier et al.*, 2002]. Although possibly continuous, the length of an X line at the magnetopause may vary. Ionosphere signatures of magnetopause reconnection suggest the length, or local time extent of an X line can vary, possibly due to solar wind drivers or the boundary conditions of the magnetopause current sheet [*Milan et al.*, 2016].

Within global MHD models an extended X line or magnetic separator is commonly reported. Studies designed to identify the position and extent of an X line in MHD have employed a number of techniques such as identifying a separator where magnetic topologies meet [*Laitinen et al.*, 2007; *Dorelli and Bhattacharjee*, 2008; *Komar et al.*, 2013; *Hoilijoki et al.*, 2014] and monitoring where magnetosheath magnetic field lines convect through the magnetopause boundary [*Ouellette et al.*, 2010]. This extended reconnection may be in the form of a single line, or it may be a line that bifurcates and recombines [*Glocer et al.*, 2016]. A consistent feature in these models is that reconnection occurs continuously across the dayside magnetopause.

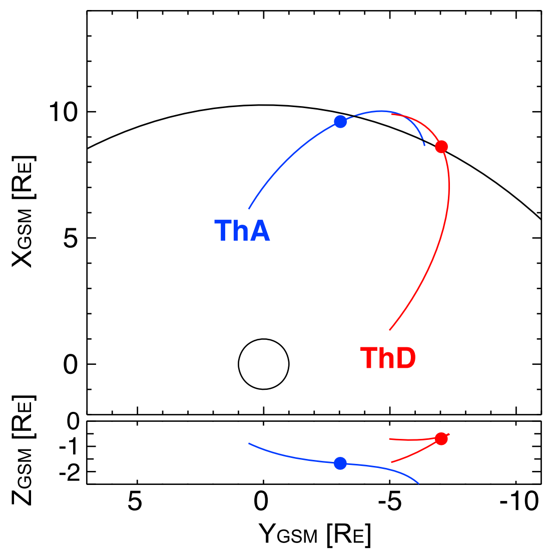

Figure 1. Orbit of the ThA and ThD spacecraft on 21 April 2014 in GSM coordinates. The solid circle indicates the locations where the spacecraft encounter the magnetopause near 11:55 UT. The magnetopause is drawn from the *Shue et al.* [1998] model.

Alternatively, reconnection could occur over an extended region but in discontinuous patches along a current sheet [*Shay et al.*, 2003]. *Alexeev et al.* [1998] suggested reconnection may be initiated by a localized current density-driven instability and could occur in multiple patches along the dayside magnetopause. Flux transfer events (FTEs) generated by bursts of localized reconnection [*Russell and Elphic*, 1979] may also be consistent with spatially localized patches or discontinuous reconnection occurring over an extended region. Patchy and spatially localized reconnection has been suggested to describe the nature of reconnection in a number of regions including the magnetopause [*Newell and Meng*, 1991] as well as the solar corona [*Linton and Longcope*, 2006]. A connection between a localized patch of reconnection and a long extended X line may come in X line spreading. Perhaps reconnection is initiated in a patch and spreads to a larger extended X line [e.g., *Milan et al.*, 2000; *Huba and Rudakov*, 2002; *Lapenta et al.*, 2006].

Reconnection could also occur in the form of multiple extended X lines. The presence of multiple X lines along the dayside magnetopause with similar local times and different latitudes was initially proposed as a generation mechanism for flux transfer events (FTEs) [*Lee and Fu*, 1985; *Sonnerup*, 1987]. This geometry is commonly observed in global MHD [*Raeder*, 2006; *Dorelli and Bhattacharjee*, 2009] as well as hybrid simulations [*Sibeck and Omidi*, 2012; *Pfau-Kempf et al.*, 2016]. It has also been observed in a number of spacecraft measurements [*Hasegawa et al.*, 2010; *Øieroset et al.*, 2011; *Zhang et al.*, 2012; *Wilder et al.*, 2014].

In this paper, spacecraft measurements from the Time History of Events and Macroscale Interactions during Substorms (THEMIS) mission are analyzed to estimate the local time extent of magnetopause reconnection. The spacecraft measurements are placed into the context of conceptual models for comparison and support reconnection occurring as either an X line with a limited spatial extent or one that is spatially discontinuous and patchy in nature.

2. Multipoint Measurements

Simultaneous multipoint measurements at the Earth's dayside magnetopause were made by the THEMIS (Th)A and ThD spacecraft [*Angelopoulos*, 2008] on 21 April 2014. The two spacecraft were on the dayside, dawn of local noon with 3.9 R_E spatial separation, and 1.4 h separation in local time. Both spacecraft were near the magnetic equator. Figure 1 displays the orbits and location of the two spacecraft during the period of interest.

Measurements from the spacecraft are presented in Figure 2. The magnetic field values are from the fluxgate magnetometer (FGM) [*Auster et al.*, 2008], while the particle measurements and plasma moments are from the electrostatic analyzer (ESA) [*McFadden et al.*, 2008]. Onboard calculations of the plasma moments from ESA are used for analysis of both spacecraft. Bulk flow and magnetic field coordinates are presented in boundary normal coordinates (*LMN*) where *L* is along the outflow direction, *M* is along the X line, and *N* is the current sheet normal. The coordinate system was identified through minimum variance of the magnetic field (MVAB) [*Sonnerup and Cahill*, 1967]. As each spacecraft passed from the magnetosheath into the magnetosphere, the density decreased, the magnetic field rotated, and the ion spectra changed.

The density and magnetic field values in the magnetosheath were similar at the two spacecraft. The density for both spacecraft was near 10 cm^{-3} and 0.4 cm^{-3} in the magnetosheath and magnetosphere, respectively. In the magnetosheath the magnetic field was primarily in the reconnecting field direction (B_L) but with some B_M component. The spacecraft observed a magnetic field rotation of 133° and 136° at ThA and ThD, respectively. Although there were a number of similarities, the bulk flow along the magnetopause (*M* direction) was close to 100 km/s higher at ThD than at ThA. Lastly, the dipole tilt during the encounter was 15°.

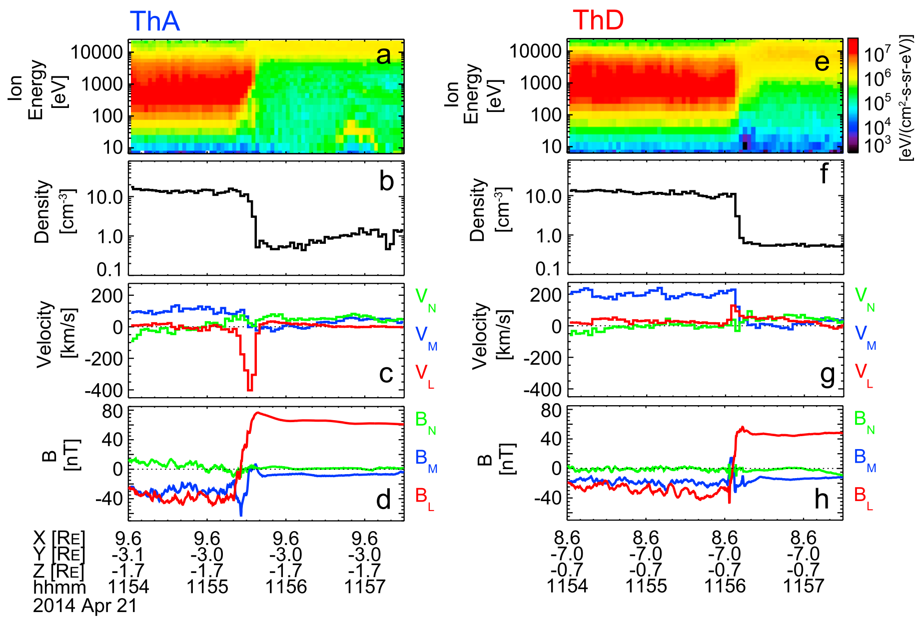

Figure 2. Measurements from ThA and ThD at the dayside magnetopause for the same 3.5 min time period. (a and e) Display ion energy spectra, (b and f) ion density, (c and g) bulk flow, and (d and h) magnetic field.

2.1. ThA: Active Magnetic Reconnection

ThA (left side of Figure 2) crosses the magnetopause boundary layer at 11:55:36 UT. While passing through the boundary, the spacecraft measures both fluid and kinetic signatures of reconnection.

$$\Delta\vec{v}_{\text{observed}} = \vec{v}_2 - \vec{v}_1 \quad (1)$$

$$\Delta\vec{v}_{\text{predicted}} = \pm\sqrt{\frac{1-\alpha_1}{\mu_0\rho_1}}\left[\vec{B}_2\left(\frac{1-\alpha_2}{1-\alpha_1}\right) - \vec{B}_1\right] \quad (2)$$

For asymmetric reconnection at the magnetopause, the largest flow acceleration occurs across the tangential discontinuity. The Walén relation (equation (2)) is based on the conservation of momentum through the boundary and describes the predicted flow from a tangential stress balance across this boundary [*Paschmann et al.*, 1986] and thus a condition which should be satisfied if reconnection is occurring. In equation (2), $\alpha = (p_{\parallel} - p_{\perp})\mu_0/B^2$ is the anisotropy factor calculated from the difference between the parallel and perpendicular pressures, where μ_0 is the magnetic permeability of vacuum and B is the magnetic field. The subscript "1" denotes the inflow side, while "2" denotes the outflow jet region. In the case of asymmetric reconnection, where the density is much greater in the magnetosheath, the inflow is primarily from the magnetosheath side [*Cassak and Shay*, 2007] which is used as value "1." The reference value from the magnetosheath was obtained from a 10 s period just outside the boundary encounter (11:54:20–11:54:30 UT).

The Walén relation provides a test of the magnitude as well as the direction of the bulk flow. The ratio between magnitude of the observed ($|\Delta\vec{v}_{\text{observed}}|$) and the predicted velocity ($|\Delta\vec{v}_{\text{predicted}}|$) is 0.9 (where 1.0 would be an exact match). The angle between the two vectors is 5°, both consistent with a reconnecting magnetopause. The observed jet in the reconnecting component is in the $-L$ direction indicating the spacecraft is "below" or south of the reconnection location.

The particle signatures are also consistent with active reconnection. As magnetosheath particles encounter newly opened magnetic field lines at the magnetopause, they can enter the magnetosphere or reflect at the boundary. In the Earth reference frame, only particles with parallel velocity greater than the de Hoffman-Teller velocity pass through the boundary. This effect results in the commonly reported "D-shaped" velocity distribution on the magnetosphere side of the boundary [*Cowley*, 1982]. The evolution of the particle distribution as the spacecraft passed through the boundary is presented in Figure 3. Figure 3 presents a similar time period as Figure 2 but includes velocity distributions during the crossing for both spacecraft. Figure 3 (bottom row)

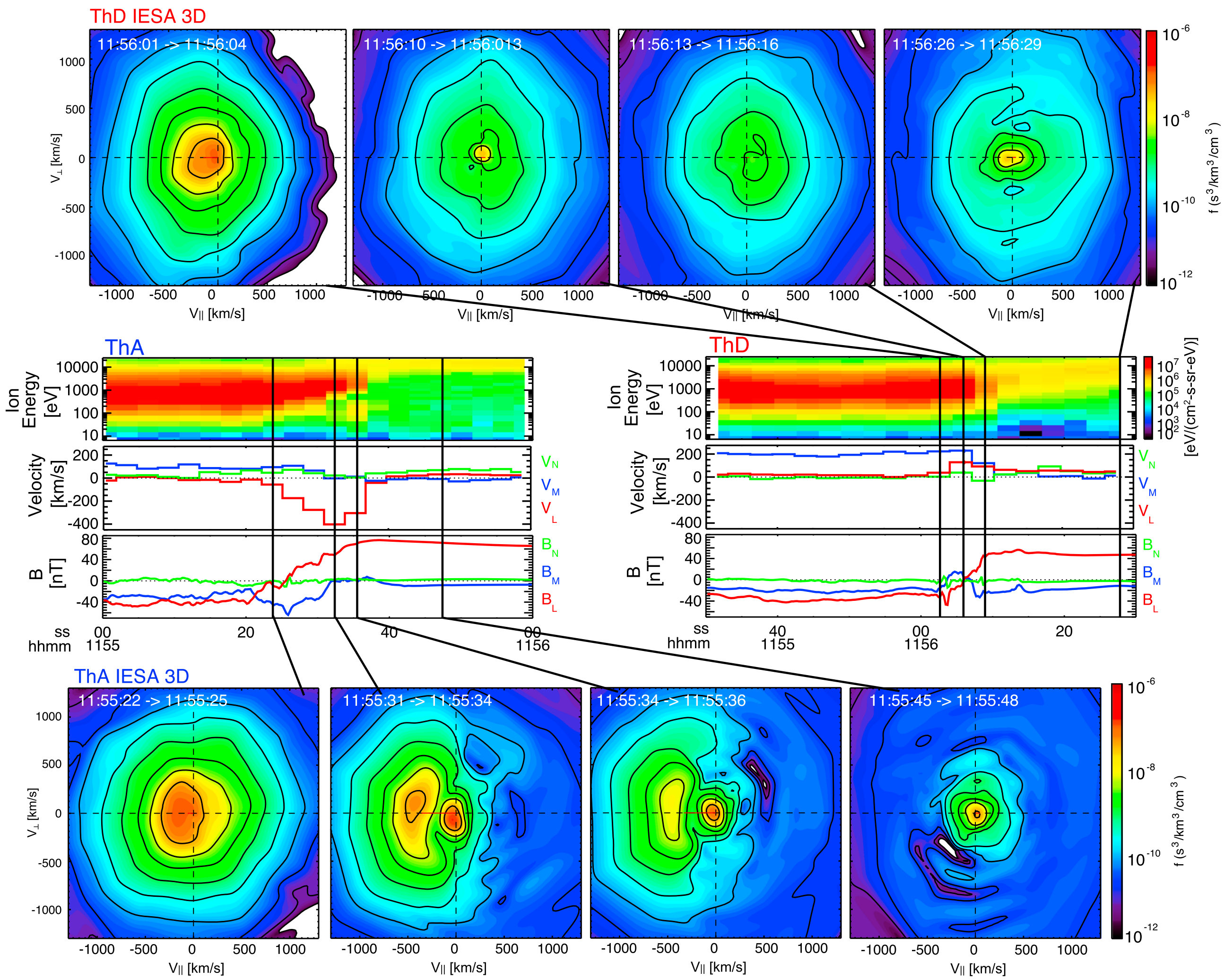

Figure 3. Observations from ThA and ThD while passing through the magnetopause are shown. The time period and format are similar to Figure 2 with ion velocity distribution functions provided. ThA observes clear D-shaped distributions.

corresponding to ThA provides clear examples of D-shaped distributions, indicative of an active reconnecting X line.

2.2. ThD: Nonreconnection Boundary

ThD passes from the magnetosheath to the magnetosphere at 11:56:07 UT, roughly 30 s after ThA. Measurements from ThD during the boundary crossing are given in Figure 2 (right). Once again the encounter is identified through changes in the ion energy spectra, a decrease in density, and a rotation of the magnetic field.

One visible difference between the two magnetopause crossing is the bulk flow at the boundary. ThA observed a clear, large-amplitude jet in the $-V_L$ direction. ThD measured a small enhancement in the $+V_L$ direction. To test whether this small enhancement may be consistent with a reconnecting boundary, the plasma parameters were once again tested with the Walén relation. The minimum angle during the crossing period between the predicted and measured velocity was 29° and corresponded to a ratio of the measured to predicted velocity magnitude of 0.2 occurring at 11:56:05. A value of 0.2 is far below the predicted flow and is not consistent with active reconnection.

A second test of the occurrence of reconnection is the velocity distribution functions. Figure 3 (top row) presents several particle distributions showing the evolution as the spacecraft passes through the boundary. The distributions transition from the dense cooler distribution in the magnetosheath to the hot, more tenuous distribution within the magnetosphere with no evidence for local magnetic reconnection. If ThD was passing very close to or through the diffusion region of the X line, one would not expect the jet velocity to have reached

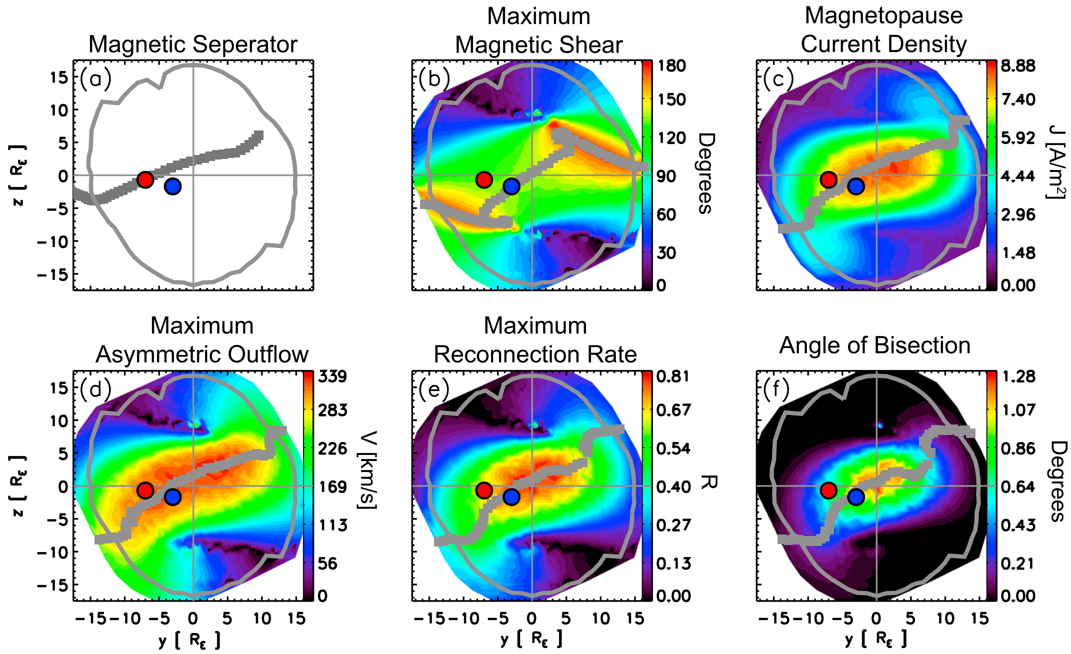

Figure 4. Predicted reconnection location positions (grey lines). The blue and red colored circles represent the positions of ThA and ThD respectively. Each panel displays the prediction from a different reconnection identifier, (a) the magnetic separator method, (b) the maximum magnetic shear, (c) magnetopause current density, (d) maximized asymmetric outflow speed, (e) maximized reconnection rate, and (f) angle of bisection models. The thinner grey line is the terminator. Plasma parameters used in the reconnection models were obtained from a BATS-R-US MHD model with observed solar wind measurements.

full speed and thus would not satisfy the Walén relation. One would, however, still expect to see signatures in the ion distribution functions [*Phan et al.*, 2016; *Burch and Phan*, 2016] which are not observed here.

Another difference between measurements at the two spacecraft is the bulk flow along the magnetopause boundary. Within the magnetosheath it is generally thought that the bulk flow approaches stagnation near the subsolar point but increases speed with distance down tail. ThA was closer to the subsolar point and observed flow along the magnetopause $V_M \approx 100$ km/s. ThD was several R_E downtail and observed $V_M \approx 200$ km/s, consistent with this understanding. Although we do not directly investigate the potential driver which may have impeded reconnection, we note that shear flows have been shown to impact the reconnection process. In the M direction, perpendicular to the reconnecting plane, flow has been shown to increase the dynamic nature of the system, potentially triggering waves along the boundary interwoven with reconnection [*Ma et al.*, 2014a, 2014b].

2.3. Model Predictions for X line Position

Predicted locations of reconnection across the magnetopause from several models were calculated for comparison with the spacecraft measurements. If the models predict reconnection to be occurring far from the position of the spacecraft, one would not anticipate to observe signatures of the process. Alternatively, if the models consistently predict reconnection to be occurring near the position of both spacecraft, it could be evidence for a spatially limited or discontinuous process since only one of the two spacecraft observes reconnection.

Figure 4 displays the results from the magnetic separator [*Komar et al.*, 2013] technique, the maximum magnetic shear [*Trattner et al.*, 2007], magnetopause current density [*Alexeev et al.*, 1998], maximized asymmetric outflow speed [*Swisdak and Drake*, 2007], maximized reconnection rate, and the angle of bisection [*Moore et al.*, 2002] reconnection models. The plasma and field parameters used for model inputs were obtained from a global Block Adaptive Tree Solarwind Roe-type Upwind Scheme (BATS-R-US) [*Powell et al.*, 1999; *Gombosi et al.*, 2000; *De Zeeuw et al.*, 2000] MHD simulation run at NASA's Community Coordinated Modeling Center (CCMC) with the Space Weather Modeling Framework[*Tóth et al.*, 2005]. Further description of the process to identify the reconnection separator for the models is provided in *Komar et al.* [2013]. The simulation was run with spacecraft observed solar wind measurements obtained from ThB sitting upstream in the solar wind and time propagated to the magnetopause, IMF B_{GSM} = [4.0, 3.3, −3.9] nT, $n = 2.0$ cm^{-3}, V = [−563, −27, 27] km/s.

Although there is some variation in the predicted locations from the models displayed in Figure 4, the locations of both ThA and ThD are within several Earth radii of each model spanning across the magnetopause. Due to the proximity, if reconnection was active along the full local time extent of the reconnection lines, one would expect a probe in the positions of the spacecraft to have measured signatures of the process. Although global MHD models have inherent limitations, the models tested provide relatively consistent predictions and the boundary crossing occurred during steady southward IMF, both supporting the idea that reconnection would be occurring along the dayside magnetopause if active. The absence of reconnection signatures at ThD indicates that reconnection was not occurring at this local time during the magnetopause boundary encounter.

3. Discussion

The spacecraft alignment and near-simultaneous magnetopause encounters allow the spatial properties of magnetic reconnection to be probed. ThA measured active reconnection along the dayside magnetopause at 10.8 h MLT. Just dawnward at 9.4 h MLT ThD observed no signatures of active reconnection. These observations provide constraints on the properties of reconnection along the dayside boundary. Several models capable of generating the observed signatures are explored in the context of the presented measurements.

3.1. Model 1: Patchy Reconnection

The first scenario is one of many discrete patches of reconnection. In this model reconnection may be active at a number of discontinuous locations or patches across the magnetopause [e.g., *Kan*, 1988; *Nishida*, 1989; *Shay et al.*, 2003]. These patches could be small and localized or have some finite extension in local time. In some places along the boundary there could be multiple patches of reconnection at similar local times but different latitudes, while at other local times there may be only a single patch giving the impression of a single X line to a localized observer. ThA measures signatures of reconnection, but 3.9 R_E away at ThD no reconnection is measured, consistent with a possible outcome from this model.

3.2. Model 2: Spatially Limited X line

Rather than discontinuous patches of reconnection as described in the previous model, reconnection could be a continuous process that only spans a short local time portion of the dayside magnetopause. In the context of these spacecraft measurements, the X line would be relatively limited in spatial extent. Using both spacecraft to constrain our estimate, and assuming reconnection extends the same distance on both sides of the subsolar point, the length L of the X line is $2.4 \leq L < 5.2$ h in local time or $6 \leq L < 14$ R_E. This result is fairly limited compared to other studies, some suggest that the magnetopause X line may span 44 R_E [*Dunlop et al.*, 2011] or 40 R_E in length [*Phan et al.*, 2000]. It should be noted that estimates of very long X lines at the magnetopause are typically based on spacecraft measurements at two points and require the assumption that reconnection is continuous between the two locations. Alternatively, reconnection could be discontinuous across the boundary, as described in the previous model, which would reduce the length of the X line significantly. It is also be noted that the assumption of reconnection being symmetric about the subsolar point is not directly based on the measurements presented but has been used in previous studies [*Phan et al.*, 2000] and allows for an estimate of the local time extent.

Although spacecraft-based studies have often found an X line at the magnetopause to be extended across large regions of the dayside or further, ground-based measurements have often led researchers to conclude reconnection may be spatially limited, extending only a few hours in local time or several R_E. Using auroral and ground-based radar measurements to determine the spatial extent of a reconnection-generated flux transfer event, *Milan et al.* [2016] found the local time extent to be 2 h, consistent with the lower end of the 2.4–5.2 h extent estimated from the measurements here. Other studies have identified flow bursts in the ionosphere corresponding to a reconnecting region and concluded these correspond to just fractions of an hour in local time at the magnetopause [*Oksavik et al.*, 2004, 2005].

3.3. Model 3: Rapid Bursts

The last model considered here describes reconnection as spatially extended but rapidly turning on and off. In this model, active reconnection spanned across the magnetopause when ThA passed through the boundary.

After the encounter by ThA, the process rapidly turned itself off before ThD arrived, roughly 30 s later. Although near simultaneous, since there is a short time difference between the two magnetopause encounters, there remains the possibility for some temporal ambiguity. One requirement of this temporal model is for reconnection to halt and for signatures to disperse in a short period of time. A second requirement of this model is that the process must be turned off due to some intrinsic property of reconnection since the solar wind, and therefore the external driving, does not introduce much variation. Steady measurements of density, inflow velocity, and magnetic field magnitude and direction were observed during this period. Although variability in the position and efficiency of reconnection is observed, even for steady inputs, for southward IMF, the "death" of an X line is typically reported to be caused by the structure convecting tailward along the magnetopause away from the subsolar point rather than switching off on the dayside magnetopause [*Sibeck and Omidi*, 2012; *Glocer et al.*, 2016; *Hoilijoki et al.*, 2017]. With a spatial separation between the two spacecraft of 3.9 R_E, and assuming the X line is moving at the speed of the magnetosheath flow (~200 km/s), it would take more than 2 min for the X line to move from ThA past ThD along the magnetopause. Since ThD encountered the magnetopause just 30 s later and did not observe active reconnection, an extended X line moving tailward is not consistent with the observations. For these reasons, we conclude that a spatial model (either Model 1 or Model 2) is more likely to describe the observations.

4. Conclusion

Multipoint spacecraft measurements are presented to study the spatial properties of magnetic reconnection. A case study is presented with two THEMIS spacecraft within the dayside magnetopause boundary layer with 3.9 R_E separation. ThA measured both fluid and kinetic signatures of magnetic reconnection, while ThD did not measure active reconnection. A comparison with several reconnection models predicted that both spacecraft were within several Earth radii of reconnection at the magnetopause indicating both should observe the process if it was indeed occurring. The measurements constrain the local length of reconnection at the magnetopause. Applying the assumption that reconnection is symmetric about the subsolar point, the extent or length L of the reconnection during this event is $2.4 \leq L < 5.2$ h in local time or $6 \leq L < 14$ R_E.

Acknowledgments
Support was given by the NASA grants NNX16AJ73G and NNX16AD91G. Support for Y.P-K. is provided by the Academy of Finland (SA-Vlasov grant 267144) and ERC consolidator grant ERC-CoG-682068-PRESTISSIMO. The authors acknowledge use of the SPEDAS analysis software. Data used in this study are openly accessible from http://themis.ssl.berkeley.edu/. Simulations were performed at the Community Coordinated Modeling Center at Goddard Space Flight Center through their public Runs on Request system (http://ccmc.gsfc.nasa.gov). The CCMC is a multiagency partnership between NASA, AFMC, AFOSR, AFRL, AFWA, NOAA, NSF, and ONR. The BATS-R-US Model was developed by the Center for Space Environment Modeling at the University of Michigan. The analysis presented here was made possible via the Kameleon software package provided by the Community Coordinated Modeling Center at NASA Goddard Space Flight Center (http://ccmc.gsfc.nasa.gov). Software Developers are M. M. Maddox, D. H. Berrios, and L. Rastaetter. The simulation data used to produce the results of this paper are publicly available for free from CCMC.

References

Alexeev, I. I., D. G. Sibeck, and S. Y. Bobrovnikov (1998), Concerning the location of magnetopause merging as a function of the magnetopause current strength, *J. Geophys. Res.*, *103*(A4), 6675–6684, doi:10.1029/97JA02863.

Angelopoulos, V. (2008), The THEMIS mission, *Space Sci. Rev.*, *141*, 5–34, doi:10.1007/s11214-008-9336-1.

Auster, H. U., et al. (2008), The THEMIS fluxgate magnetometer, *Space Sci. Rev.*, *141*, 235–264.

Burch, J. L., and T. D. Phan (2016), Magnetic reconnection at the dayside magnetopause: Advances with MMS, *Geophys. Res. Lett.*, *43*, 8327–8338, doi:10.1002/2016GL069787.

Cassak, P. A., and M. A. Shay (2007), Scaling of asymmetric magnetic reconnection: General theory and collisional simulations, *Phys. Plasmas*, *14*(10), 102114, doi:10.1063/1.2795630.

Cowley, S. W. H. (1982), The causes of convection in the Earth's magnetosphere: A review of developments during the IMS, *Rev. Geophys.*, *20*(3), 531–565, doi:10.1029/RG020i003p00531.

De Zeeuw, D., T. Gombosi, C. Groth, K. Powell, and Q. Stout (2000), An adaptive MHD method for global space weather simulations, *IEEE Trans. Plasma Sci.*, *28*, 1956–1965, doi:10.1109/27.902224.

Dorelli, J. C., and A. Bhattacharjee (2008), Defining and identifying three-dimensional magnetic reconnection in resistive magnetohydrodynamic simulations of Earth's magnetosphere, *Phys. Plasmas*, *15*, 056504, doi:10.1063/1.2913548.

Dorelli, J. C., and A. Bhattacharjee (2009), On the generation and topology of flux transfer events, *J. Geophys. Res.*, *114*, A06213, doi:10.1029/2008JA013410.

Dunlop, M. W., et al. (2011), Magnetopause reconnection across wide local time, *Ann. Geophys.*, *29*, 1683–1697.

Fuselier, S. A., H. U. Frey, K. J. Trattner, S. B. Mende, and J. L. Burch (2002), Cusp aurora dependence on interplanetary magnetic field B_z, *J. Geophys. Res.*, *107*(A7), 1111, doi:10.1029/2001JA900165.

Glocer, A., J. Dorelli, G. Toth, C. M. Komar, and P. A. Cassak (2016), Separator reconnection at the magnetopause for predominantly northward and southward IMF: Techniques and results, *J. Geophys. Res. Space Physics*, *121*, 140–156, doi:10.1002/2015JA021417.

Gombosi, T., D. DeZeeuw, C. Groth, and K. Powell (2000), Magnetospheric configuration for Parker-spiral IMF conditions: Results of a 3D AMR MHD simulation, *Adv. Space Res.*, *26*, 139–149, doi:10.1016/S0273-1177(99)01040-6.

Gosling, J. T., S. Eriksson, T. D. Phan, D. E. Larson, R. M. Skoug, and D. J. McComas (2007a), Direct evidence for prolonged magnetic reconnection at a continuous X-line within the heliospheric current sheet, *Geophys. Res. Lett.*, *34*, L06102, doi:10.1029/2006gl029033.

Gosling, J. T., S. Eriksson, L. M. Blush, T. D. Phan, J. G. Luhmann, D. J. McComas, R. M. Skoug, M. H. Acuna, C. T. Russell, and K. D. Simunac (2007b), Five spacecraft observations of oppositely directed exhaust jets from a magnetic reconnection X-line extending 4.26×10^6 km in the solar wind at 1 AU, *Geophys. Res. Lett.*, *34*, L20108, doi:10.1029/2007GL031492.

Hasegawa, H., et al. (2010), Evidence for a flux transfer event generated by multiple X-line reconnection at the magnetopause, *Geophys. Res. Lett.*, *37*, L16101, doi:10.1029/2010GL044219.

Hasegawa, H., et al. (2016), Decay of mesoscale flux transfer events during quasi-continuous spatially extended reconnection at the magnetopause, *Geophys. Res. Lett.*, *43*, 4755–4762, doi:10.1002/2016GL069225.

Hoilijoki, S., V. M. Souza, B. M. Walsh, P. Janhunen, and M. Palmroth (2014), Magnetopause reconnection and energy conversion as influenced by the dipole tilt and the IMF B_x, *J. Geophys. Res. Space Physics*, *119*, 4484–4494, doi:10.1002/2013JA019693.

Hoilijoki, S., U. Ganse, Y. Pfau-Kempf, P. A. Cassak, B. M. Walsh, H. Hietala, S. von Alfthan, and M. Palmroth (2017), Reconnection rates and X-line motion at the magnetopause: Global 2D-3V hybrid-Vlasov simulation results, *J. Geophys. Res. Space Physics*, *122*, doi:10.1002/2016JA023709, in press.

Huba, J. D., and L. I. Rudakov (2002), Three-dimensional Hall magnetic reconnection, *Phys. Plasmas*, *9*, 4435–4438.

Kan, J. R. (1988), A theory of patchy and intermittent reconnections for magnetospheric flux transfer events, *J. Geophys. Res.*, *93*(A6), 5613–5623, doi:10.1029/JA093iA06p05613.

Komar, C. M., P. A. Cassak, J. C. Dorelli, A. Glocer, and M. M. Kuznetsova (2013), Tracing magnetic separators and their dependence on IMF clock angle in global magnetospheric simulations, *J. Geophys. Res. Space Physics*, *118*, 4998–5007, doi:10.1002/jgra.50479.

Lapenta, G., D. Krauss-Varban, H. Karimabadi, J. D. Huba, L. I. Rudakov, and P. Ricci (2006), Kinetic simulations of X-line expansion in 3D reconnection, *Geophys. Res. Lett.*, *33*, L10102, doi:10.1029/2005GL025124.

Laitinen, T. V., M. Palmroth, T. I. Pulkkinen, P. Janhunen, and H. E. J. Koskinen (2007), Continuous reconnection line and pressure-dependent energy conversion on the magnetopause in a global MHD model, *J. Geophys. Res.*, *112*, A11201, doi:10.1029/2007JA012352.

Lee, L. C., and Z. F. Fu (1985), A theory of magnetic flux transfer at the Earth's magnetopause, *Geophys. Res. Lett.*, *12*(2), 105–108, doi:10.1029/GL012i002p00105.

Linton, M. G., and D. W. Longcope (2006), A model for patchy reconnection in three dimensions, *Astrophys. J.*, *642*(2), 1177–1192.

Ma, X., A. Otto, and P. A. Delamere (2014a), Interaction of magnetic reconnection and Kelvin-Helmholtz modes for large magnetic shear: 1. Kelvin-Helmholtz trigger, *J. Geophys. Res. Space Physics*, *119*, 781–797, doi:10.1002/2013JA019224.

Ma, X., A. Otto, and P. A. Delamere (2014b), Interaction of magnetic reconnection and Kelvin-Helmholtz modes for large magnetic shear: 2. Reconnection trigger, *J. Geophys. Res. Space Physics*, *119*, 808–820, doi:10.1002/2013JA019225.

McFadden, J. P., C. W. Carlson, D. Larson, M. Ludlam, R. Abiad, B. Elliott, P. Turin, M. Marckwordt, and V. Angelopoulos (2008), The THEMIS ESA plasma instrument and in-flight calibration, *Space Sci. Rev.*, *141*, 277–302, doi:10.1007/s11214-008-9440-2.

Milan, S. E., M. Lester, S. W. H. Cowley, and M. Brittnacher (2000), Convection and auroral response to a southward turning of the IMF: Polar UVI, CUTLASS, and IMAGE signatures of transient magnetic flux transfer at the magnetopause, *J. Geophys. Res.*, *105*(A7), 15,741–15,755, doi:10.1029/2000JA900022.

Milan, S. E., S. M. Imber, J. A. Carter, M.-T. Walach, and B. Hubert (2016), What controls the local time extent of flux transfer events?, *J. Geophys. Res. Space Physics*, *121*, 1391–1401, doi:10.1002/2015JA022012.

Moore, T. E., M.-C. Fok, and M. O. Chandler (2002), The dayside reconnection X line, *J. Geophys. Res.*, *107*(A10), 1332, doi:10.1029/2002JA009381.

Nishida, A. (1989), Can random reconnection on the magnetopause produce the low latitude boundary layer?, *Geophys. Res. Lett.*, *61*, 227–230, doi:10.1029/GL016i003p00227.

Newell, P. T., and C. I. Meng (1991), Ion acceleration at the equatorward edge of the cusp: Low altitude observations of patchy merging, *Geophys. Res. Lett.*, *18*, 1829–1832, doi:10.1029/91GL02088.

Øieroset, M., et al. (2011), Direct evidence for a three-dimensional magnetic flux rope flanked by two active magnetic reconnection X lines at Earth's magnetopause, *Phys. Rev. Lett.*, *107*(16), 65007, doi:10.1103/physrevlett.107.165007.

Oksavik, K., J. Moen, and H. C. Carlson (2004), High-resolution observations of the small-scale flow pattern associated with a poleward moving auroral form in the cusp, *Geophys. Res. Lett.*, *31*, L11807, doi:10.1029/2004GL019838.

Oksavik, K., J. Moen, H. C. Carlson, R. A. Greenwald, S. E. Milan, M. Lester, W. F. Denig, and R. J. Barnes (2005), Multi-instrument mapping of the small-scale flow dynamics related to a cusp auroral transient, *Ann. Geophys.*, *23*, 2657–2670.

Ouellette, J. E., B. N. Rogers, M. Wiltberger, and J. G. Lyon (2010), Magnetic reconnection at the dayside magnetopause in global Lyon-Fedder-Mobarry simulations, *J. Geophys. Res.*, *115*, A08222, doi:10.1029/2009ja014886.

Paschmann, G., W. Baumjohann, N. Sckopke, I. Papamastorakis, C. W. Carlson, B. U. Ö. Sonnerup, and H. Lühr (1986), The magnetopause for large magnetic shear: AMPTE/IRM observations, *J. Geophys. Res.*, *91*, 11,099–11,115.

Pfau-Kempf, Y., H. Hietala, S. E. Milan, L. Juusola, S. Hoilijoki, U. Ganse, S. von Alfthan, and M. Palroth (2016), Evidence for transient, local ion foreshocks caused by dayside magnetopause reconnection, *Ann. Geophys.*, *34*, 1943–959.

Phan, T. D., et al. (2000), Extended magnetic reconnection at the Earth's magnetopause from detection of bi-directional jets, *Nature*, *404*(6780), 848–850, doi:10.1038/35009050.

Phan, T. D., et al. (2006a), A magnetic reconnection X-line extending more than 390 Earth radii in the solar wind, *Nature*, *439*(7073), 175–178, doi:10.1038/nature04393.

Phan, T. D., H. Hasegawa, M. Fujimoto, M. Øieroset, T. Mukai, R. P. Lin, and W. Paterson (2006b), Simultaneous Geotail and Wind observations of reconnection at the subsolar and tail flank magnetopause, *Geophys. Res. Lett.*, *33*, L09104, doi:10.1029/2006GL025756.

Phan, T. D., et al. (2016), Ion Larmor radius effects near a reconnection X line at the magnetopause: THEMIS observations and simulation comparison, *Geophys. Res. Lett.*, *43*, 8844–8852, doi:10.1002/2016GL070224.

Powell, K. G., P. L. Roe, T. J. Linde, T. I. Gombosi, and D. L. D. Zeeuw (1999), A solution-adaptive upwind scheme for ideal magnetohydrodynamics, *J. Comput. Phys.*, *154*, 284–309, doi:10.1006/jcph.1999.6299.

Raeder, J. (2006), Flux transfer events: 1. Generation mechanism for strong southward IMF, *Ann. Geophys.*, *24*(1), 381–392.

Russell, C. T., and R. C. Elphic (1979), ISEE observations of flux transfer events at the dayside magnetopause, *Geophys. Res. Lett.*, *6*(1), 33–36, doi:10.1029/GL006i001p00033.

Shay, M. A., J. F. Drake, M. Swisdak, W. Dorland, and B. N. Rogers (2003), Inherently three-dimensional magnetic reconnection: A mechanism for bursty bulk flows?, *Geophys. Res. Lett.*, *30*(6), 1345, doi:10.1029/2002GL016267.

Shue, J.-H., et al. (1998), Magnetopause location under extreme solar wind conditions, *J. Geophys. Res.*, *103*, 17,691–17,710, doi:10.1029/98JA01103.

Sibeck, D. G., and N. Omidi (2012), Flux transfer events: Motion and signatures, *J. Atmos. Terr. Phys.*, *87–88*, 20–24, doi:10.1016/j.jastp.2011.07.010.

Sonnerup, B. U. Ö. (1987), On the stress balance in flux transfer events, *J. Geophys. Res.*, *92*, 8613–8620.

Sonnerup, B. U. Ö., and L. J. Cahill Jr. (1967), Magnetopause structure and attitude from Explorer 12 observations, *J. Geophys. Res.*, *72*(1), 171–183, doi:10.1029/JZ072i001p00171.

Swisdak, M., and J. F. Drake (2007), Orientation of the reconnection X-line, *Geophys. Res. Lett.*, *34*, L11106, doi:10.1029/2007GL029815.

Tóth, G., et al. (2005), Space Weather Modeling Framework: A new tool for the space science community, *J. Geophys. Res.*, *110*, A12226, doi:10.1029/2005JA011126.

Trattner, K. J., J. S. Mulcock, S. M. Petrinec, and S. A. Fuselier (2007), Probing the boundary between antiparallel and component reconnection during southward interplanetary magnetic field conditions, *J. Geophys. Res.*, *112*, A08210, doi:10.1029/2007JA012270.

Walsh, B. M., T. D. Phan, D. G. Sibeck, and V. M. Souza (2014), The plasmaspheric plume and magnetopause reconnection, *Geophys. Res. Lett.*, *41*, 223–228, doi:10.1002/2013GL058802.

Wilder, F. D., S. Eriksson, K. J. Trattner, P. A. Cassak, S. A. Fuselier, and B. Lybekk (2014), Observation of a retreating X line and magnetic islands poleward of the cusp during northward interplanetary magnetic field conditions, *J. Geophys. Res. Space Physics*, *119*, 9643–9657, doi:10.1002/2014JA020453.

Zhang, H., M. G. Kivelson, V. Angelopoulos, K. K. Khurana, Z. Y. Pu, R. J. Walker, R. L. McPherron, T. S. Hsu, Q. G. Zong, and T. D. Phan (2012), Generation and properties of in vivo flux transfer events, *J. Geophys. Res.*, *117*, A05224, doi:10.1029/2011JA017166.